

Document downloaded from:

<http://hdl.handle.net/10251/183770>

This paper must be cited as:

García Martínez, A.; Monsalve-Serrano, J.; Lago-Sari, R.; Fogué-Robles, Á. (2021). Use of EGR e-pump for Dual-Mode Dual-Fuel engines in mild hybrid architectures. *Energy Conversion and Management*. 247:1-13. <https://doi.org/10.1016/j.enconman.2021.114701>



The final publication is available at

<https://doi.org/10.1016/j.enconman.2021.114701>

Copyright Elsevier

Additional Information

1 **Use of EGR e-Pump for Dual-Mode Dual-Fuel Engines in Mild Hybrid Architectures**

2
3 **Antonio García, Javier Monsalve-Serrano* , Rafael Lago Sari, Álvaro Fogué-Robles**

4
5 CMT - Motores Térmicos, Universitat Politècnica de València, Camino de Vera s/n,
6 46022 Valencia, Spain

7
8 Energy Conversion and Management

9 Volume 247, 1 November 2021, 114701

10 <https://doi.org/10.1016/j.enconman.2021.114701>

11
12
13 Corresponding author (*):

14 Dr. Javier Monsalve-Serrano (jamonse1@mot.upv.es)

15 Phone: +34 963876559

16
17
18 **Abstract**

19 Highway transport sector is still expected to be dominated by internal combustion
20 engines in the future, especially due to limitations in the introduction and applicability
21 of full electrification for heavy-duty propulsive systems. Nonetheless, this sector is still
22 under the objectives imposed in the roadmap towards carbon neutrality. For this, engine
23 efficiency and low-emission combustion modes must be improved, and the introduction
24 of synthetic fuels, low electrification levels and devices for engine optimization and
25 energy management have proven to be a great advance towards these objectives. This
26 work studies the application of an EGR e-pump for energy recovery and combustion
27 optimization on a powertrain running on Dual-Mode Dual-Fuel combustion mode as a
28 substitute of a complex dual route EGR system. The results include the evaluation of the
29 impact of using energy recovery devices on combustion performance and emissions
30 levels, as well as a numerical evaluation of driving conditions considering a medium-duty
31 application in the transport sector under different driving scenarios. The results point
32 out that the inclusion of the EGR e-pump can contribute to mitigate the drawbacks of
33 removing the complex dual route system in terms of equivalent fuel consumption
34 without greater impact in terms of emissions. Additionally, its application in mild hybrid
35 platforms can promote a significant improvement in CO₂ emissions, especially for urban
36 areas (20% compared to a conventional powertrain based on HP EGR).

37 **Keywords**

38 Powertrain electrification; EGR e-pump, advanced air management systems; Dual-
39 Mode Dual-Fuel combustion; Mild hybrid trucks.

40

41 1. Introduction

42 Carbon neutrality is the ultimate goal to be obtained in the next few years ahead to fulfil
43 with the green deal agreed by the G7 nations [1]. This imposes several restrictions
44 concerning the road transportation sector since it represents a share of $\approx 12\%$ in the total
45 CO₂ produced globally [2]. In Europe, this is even more relevant since the road
46 transportation share increases up to 18% [3]. While battery electric vehicles are gaining
47 attention as a possible solution for light-duty transport [4], the decarbonization of
48 heavy-duty transportation has no clear solution. The usage profile and energetic
49 demand of heavy-duty applications leads to several barriers regarding the full
50 electrification of this sector [5]. The significant reduction in the truck payload ($\approx 20\%$),
51 long charging times and increased total cost of ownership are some of the problems that
52 hinders the use of BEVs for heavy-duty applications. On the other hand, hydrogen-
53 fuelled engines seem to be an alternative, since it provides zero CO₂ emissions in a tank
54 -to-wheel basis, with reduced barriers for its introduction [6]. Nonetheless, this fuel still
55 lags with respect to conventional fuels in its distribution infrastructure and requires
56 dedicated powertrain design [7]. A mid-term solution could be the use of hydrogen-
57 derived fuels with similar characteristics than those of conventional fuels, enabling the
58 use of the current powertrain and distribution systems [8][9]. Clearly, the benefits would
59 be reduced since higher energy demand is required to process hydrogen to fuels such
60 as e-diesel and e-gasoline. Nonetheless, these fuels can be produced outside the country
61 where they are consumed, benefiting from places where renewable energy is found in
62 abundance such as Chile, Kingdom of Saudi Arabia, etc. This allows to reduce the Capital
63 Expenditure (CAPEX) of the production system while having no operating expenses
64 (OPEX), which enables to compensate the lower efficiency that these fuels could have
65 compared to direct electrification [10][11].

66 Such scenario is favourable to further investigate alternatives to improve the efficiency
67 of internal combustion engines, which could favour the prompt transport
68 decarbonization by means of e-fuels [12]. Concerning the recent advances on high
69 efficiency combustion, low-temperature combustion concepts have demonstrated in
70 the past the capacity to provide higher efficiency than conventional diesel combustion
71 while attaining ultra-low soot and nitrogen oxides (NO_x) [13][14]. Several of the early
72 challenges regarding combustion controllability and load extension have been dealt
73 during the last years, attaining solutions that reached technology readiness levels (TRL)
74 up to five [15]. One of the most promising solutions is the Dual-Mode Dual-Fuel
75 combustion concept [16]. This combustion mode relies on the former Reactivity
76 Controlled Compression Ignition combustion (RCCI) in a great extent (from low to
77 medium load) [17]. Nonetheless, additional stratification paths are added to the
78 combustion chamber whenever the operation starts to be limited by pressure gradients.
79 The most effective strategy is to increase the equivalence ratio stratification by means
80 of shifting the high-reactivity fuel injection towards the top dead center, allowing to
81 extend the engine operational range up to full load conditions [18]. This requires an
82 increase in the oxygen concentration while maintaining the EGR levels, to avoid soot and
83 NO_x formation. Nonetheless, this implies a wide range of mass flows through the turbine
84 and compressor which are not possible to be achieved by conventional turbochargers,
85 since they either operates near to the surge or the choke zones. Recently, these
86 limitations started to be overcome by introducing mild hybrid electrification in the

87 vehicles [19]. This has enabled the use of electrified air management systems such as e-
88 Pumps for EGR and e-turbochargers [20][21]. Both devices allow to decouple the
89 dependence of the air management system on the exhaust energy. Recent studies
90 carried out by Smith [22] in a 4-cylinder heavy-duty engine representative of call 8 trucks
91 have highlighted the potential of the EGR e-pump in providing the required EGR
92 concentrations for NO_x control while enabling the simplification of the air management
93 system from variable geometry turbines (VGT) to fixed geometry turbines (FGT). García
94 et al. [21] also performed a numerical investigation aiming at identifying the benefits
95 and challenges of using electrified air management systems such as EGR e-pump and e-
96 turbocharger in a mild hybrid vehicle. The simulation results allowed to conclude that
97 the combination of the system allows both fuel consumption savings and simplification
98 of the geometry towards a fixed geometry turbine. Additionally, it was suggested that
99 the use of e-pump allows to reduce the transient response of EGR while enabling energy
100 recuperation in specific cases.

101 Despite the potential of this system, there are only few works available in the literature.
102 In addition, they are fully based on numerical assessments and focused exclusively on
103 consumption and emission investigations. Nonetheless, it is believed that experimental
104 investigations need to be carried to investigate not only performance and emissions
105 parameters but also the complex interplay that the EGR e-pump may introduce in the
106 system regarding combustion, fuel injection and air management. Additionally, the
107 extension of this investigation towards a full map calibration is mandatory to draw the
108 complete scenario of this system as a potential solution for electrified powertrains. In
109 this sense, this investigation aims at evaluating the application of an e-pump EGR system
110 in combination with an advanced low temperature combustion concept as a pathway to
111 deliver a clean and efficient powertrain solution to comply with the regulations that are
112 to come. Experimental assessments are performed in a multi-cylinder engine platform,
113 previously modified to run under DMDF combustion. A prototype e-pump EGR system
114 was included to the engine fed by a 48 V power source system, allowing to monitor and
115 quantify the energy conversion and management of the different power sources. This
116 means that the possible energy recovery and its conversion to electrical energy can be
117 assessed as well as the energy needed to deliver the required EGR amount can be also
118 quantified. The investigations were performed first at representative conditions by
119 applying parametric studies to assess the impact of the e-pump EGR system on the
120 energy management and the combustion process. Next, considering the conclusions
121 from the first investigation, a full map calibration was sought followed by a driving cycle
122 evaluation. The last was performed considering a mild-hybrid 48 V vehicle platform to
123 attain a real scenario in terms of the benefits that may be obtained combined mild-
124 hybridization and the EGR e-pump.

125

126 **2. Experimental materials and methodology**

127 This section intends to detail the engine and experimental facility employed during this
128 investigation as well as the EGR e-pump description, heat exchanger configuration and
129 the testing methodology developed to carry out this work.

130 **2.1. Engine and test cell facility description**

131 Air management performance is highly dependent on the thermodynamic conditions
 132 that are found in the inlet and outlet of compressor and turbine. Low temperature
 133 combustion concepts have particularities such as low exhaust gas temperatures and
 134 high exhaust recirculation levels, which may decrease the energy availability for the
 135 turbine [23]. In this sense, the real representation of this boundary conditions is of
 136 utmost importance. One of the most representative way to account the limitations and
 137 the conditions that may be found in the system is by means of multi-cylinder engine
 138 testing. Therefore, this evaluation was performed using a multi-cylinder engine,
 139 representative of medium-duty applications. This engine was calibrated in the past for
 140 a Dual-Mode Dual-Fuel combustion having different targets such as EUVI NO_x [24][25].
 141 In addition, it has a combustion system optimized for this concept [26]. The main
 142 characteristics of the engine are presented in Table 1.

143

Table 1. Main engine characteristics.

Engine Characteristics	
Engine Type	4 stroke, 4 valves, direct injection
Number of cylinders [-]	6
Displaced volume [cm ³]	7700
Stroke [mm]	135
Bore [mm]	110
Piston bowl geometry [-]	Bathtub
Compression ratio [-]	12.75:1
Rated power [kW]	235 @ 2100 rpm
Rated torque [Nm]	1200 @ 1050-1600 rpm

144

145 This engine has been modified to enable its operation in DMDF mode. First, the original
 146 compression engine was reduced from 17.5:1 to 12.75:1 by means of piston machining.
 147 Additionally, six port fuel injectors were added to deliver the low reactivity fuel. More
 148 detail about fuel injection systems that are used in the engine and previous calibrations
 149 can be found in previous works. A fully instrumented test cell facility was used to
 150 perform this investigation. An AVL active dynamometer with an embedded PUMA
 151 system was used to control the load and engine speed for each operating condition.

152 Specific instrumentation for instantaneous in-cylinder pressure measurement, gas
 153 analysis, etc. were also included. A detailed description on the test cell instrumentation
 154 and devices that were used can be obtained in previous works from the authors [27].
 155 Table 2 summarizes the different sensors used and their associate accuracy. The
 156 addition of the EGR e-pump system required some modifications with respect to the
 157 base experimental setup. First, a heat exchanger was added prior to the e-pump EGR
 158 system to avoid excessive temperatures at the pump inlet. Additionally, specific control
 159 systems were added to the LabVIEW routine aiming at regulating the pump speed
 160 according to the operating condition required. Figure 1 illustrates the experimental
 161 facility used in this investigation.

162

163

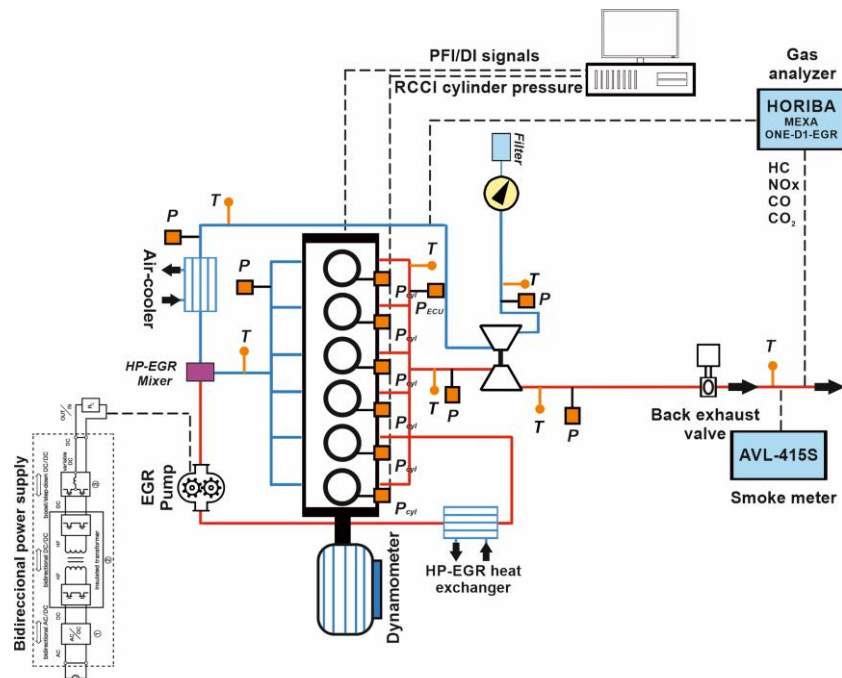
164

165

Table 2. Accuracy of the instrumentation used in this work.

Variable measured	Device	Manufacturer / model	Accuracy
In-cylinder pressure	Piezoelectric transducer	Kistler / 6125C	± 1.25 bar
Intake/exhaust pressure	Piezoresistive transducers	Kistler / 4045A	± 25 mbar
Temperature in settling chambers and manifolds	Thermocouple	TC direct / type K	± 2.5 °C
Crank angle, engine speed	Encoder	AVL / 364	± 0.02 CAD
NO _x , CO, HC, O ₂ , CO ₂	Gas analyser	HORIBA / MEXA 7100 DEGR	4%
FSN	Smoke meter	AVL / 415	± 0.025 FSN
Gasoline/diesel fuel mass flow	Fuel balances	AVL / 733S	$\pm 0.2\%$
Air mass flow	Air flow meter	Elster / RVG G100	$\pm 0.1\%$

166



167

168

Figure 1. Schematic of the equipment used in the experimental facility.

169

2.2. EGR systems considerations

170

This section describes the different EGR system configurations that have been evaluated in the current engine with DMDF combustion up to arrive to the EGR e-pump solution.

171

172

2.2.1. Dual route EGR system

173

Dual route EGR systems are composed by a low pressure EGR and high pressure EGR route. The high pressure EGR is derived before the turbine inlet while the low-pressure EGR system is taken after the turbine, passing through a set of heat exchanger and dryer to avoid water to enter in contact with the compressor blades. This system provides benefits regarding the maximum quantity of EGR that can be done, the temperatures achieved at the cylinder inlet and the pumping losses required to drive the EGR [28].

174

175

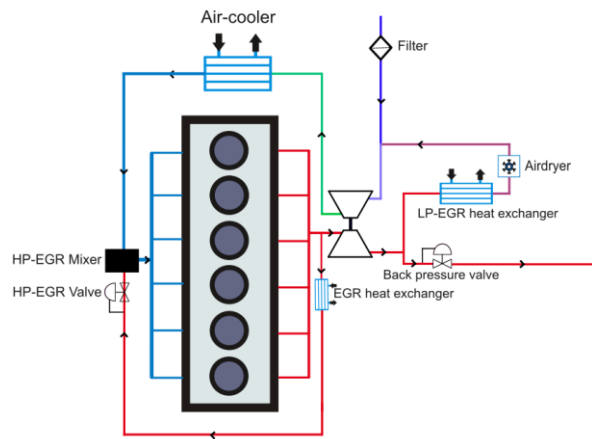
176

177

178

179 Due to these advantages, this system has been investigated for low temperature
 180 combustion concepts where high EGR concentrations are required. Figure 2 illustrates
 181 the EGR system layout that was used in the early investigations of the DMDF combustion
 182 concept, which allowed to obtain engine-out tailpipe EUVI NO_x emissions with ultra-low
 183 soot emissions and similar efficiency as the one from the original diesel calibration.

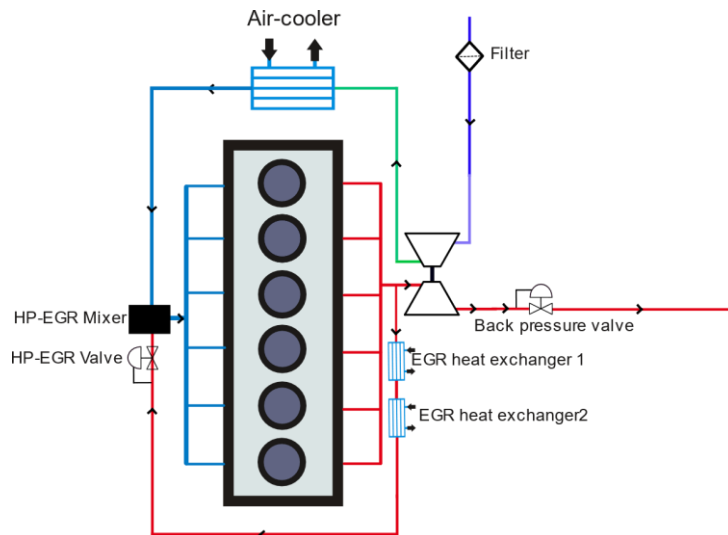
184 Despite the benefits, dual-route EGR systems present some practical challenges. One of
 185 the most important one to be considered is the packaging issue due to the space
 186 required to accommodate all the pipes, dryer, and heat exchanger for the system. Apart
 187 from that, dual-route EGR systems also lead to higher costs, being not the preferred
 188 option for wide-scale applications.



189
 190 Figure 2. Diagram of the setup used with the dual-route EGR architecture.

191 **2.2.2. High pressure EGR**

192 High pressure EGR is the simplest way to increase the dilution levels in the combustion
 193 chamber. The exhaust gas is derived before the turbine and directed towards the intake
 194 manifold, where its flow rate is regulated by means of an electric valve. The maximum
 195 EGR output is highly dependent on the pressure difference between the exhaust and
 196 intake pressure [29]. Due to its simplicity, this EGR system equips most of the current
 197 engines, including the commercial version of the engine used in this investigation.
 198 Figure 3 depicts the EGR scheme that was used in this investigation.



199

200

Figure 3. Diagram of the setup used with the HP EGR architecture.

201

2.2.3. e-Pump EGR system

202

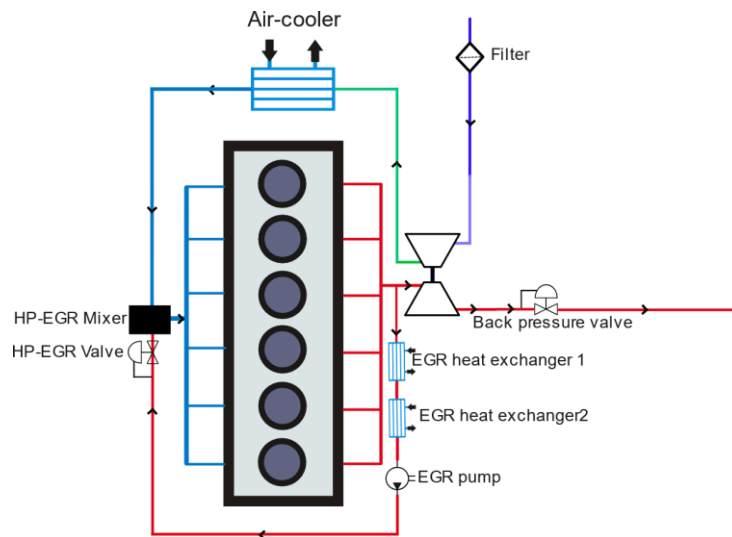
Considering the points referred in the introduction section, it is clear that the e-pump based EGR system can deliver benefits in conventional applications such as the decrease of transient times and the possibility of recovering energy from the exhaust gases in specific operating conditions. In spite of the limited capacity of the system, numerical investigations have demonstrated up to 2% of improvement in the fuel consumption using this system [21]. For this investigation, a prototype e-pump EGR system was used [30], with the specifications presented in Table 3.

209

Table 3. Technical specifications of the EGR e-pump.

Specification	Value
Displacement volume [c.c./rev]	400
Nominal power [kW]	6
Power supply [VDC]	48
Maximum speed [rpm]	10000
Power Recovery	Yes

210



211

212

Figure 4. Diagram of the setup used with the HP EGR and e-pump architecture.

213

2.3. Assessment methodology

214

The use of the EGR e-pump was assessed by means of both experiments and numerical simulations to understand its impact on driving cycles. In this sense, this section intends to describe the experimental and numerical methodology employed in this investigation.

218

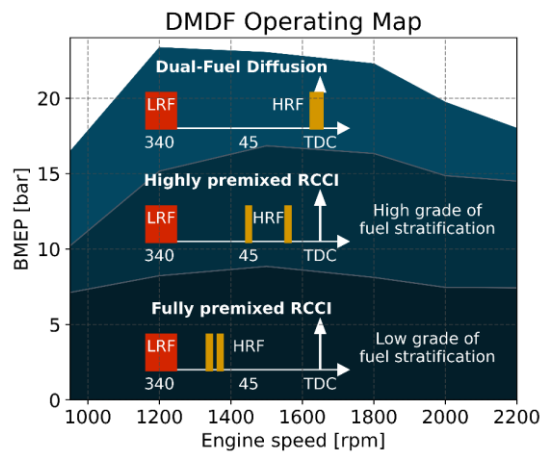
2.3.1. Experimental evaluation

219

The experimental investigations were performed in two steps. First, a parametric sweep of e-pump velocity was done in specific operating conditions. This analysis allows to understand the complex interplay among the boundary conditions in the e-pump inlet, the original air management system and the intake manifold conditions that will govern

222

223 the combustion development. The points to be assessed were chosen considering the
 224 particularities of the DMDF combustion concept. As shown in Figure 5, this concept
 225 relies on different strategies. From low to medium load, high premixing degrees are
 226 employed with low to high grade of equivalence ratio stratification. These zones also
 227 require EGR levels up to 50%. By contrast, from high to full load, a dual-fuel diffusive
 228 combustion is used, being characterized by high reactivity fuel injections near to the top
 229 dead center and EGR levels around 20%. In this sense, different engine speeds at 50% of
 230 engine load (the most demanding engine load in terms of EGR requirement) were
 231 evaluated. For each operating condition, an EGR e-pump speed sweep was performed.
 232 The limits of the sweep were experimentally determined by the points where the
 233 combustion stabilities were too high, or the e-pump started to be limited by maximum
 234 speed.



235

236

Figure 5. Conceptual injection strategy of the dual-mode dual-fuel combustion concept.

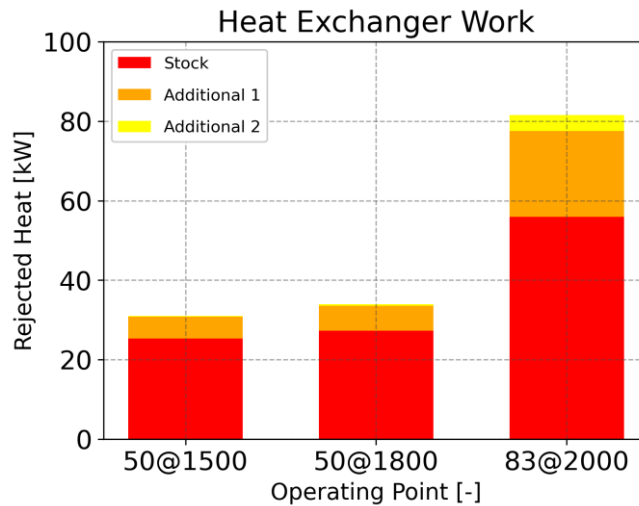
237 Next, a full map calibration is proposed, considering only the optimized operating
 238 conditions using the new system. The calibration methodology was based on that
 239 presented in previous papers such as García et al. [31] and Benajes et al. [32].
 240 Nonetheless, slight modifications were done to account for the energy spent or
 241 generated by the e-pump. This was accomplished by means of including the power signal
 242 from the e-pump to the main LabView controller interface. This signal was used to
 243 calculate a final brake specific fuel consumption according to the equation Eq. 1, which
 244 allows to include all the energy paths of the system.

$$BSFC_{eq} = \frac{\dot{m}_{LRF} \cdot \frac{LHV_{LRF}}{LHV_{LRF,ref}} + \dot{m}_{HRF} \cdot \frac{LHV_{HRF}}{LHV_{HRF,ref}}}{\dot{P}_{engine} - \dot{P}_{pump}} \quad \text{Eq. 1}$$

245 In this formula, it is considered that the power consumed or regenerated by the pump
 246 is greater than zero when EGR is being forced by the pump and it is consuming electric
 247 energy, and lower than zero for those conditions where the pump is regenerating energy
 248 and producing electric energy that is stored in the battery.

249 It is important to remark that the increase of the EGR levels that flows through the HP
 250 EGR system leads to higher demands on the heat exchanger of the original EGR system.
 251 In this sense, the cooling system needs to be redesigned to enable reasonable
 252 temperatures at the intake manifold. To do this, a specific study was performed to

253 design a cooling system for the HP-only architecture by means of an experimental
 254 characterization of the original heat exchanger and numerical simulations of the system.
 255 This has allowed to define the number of heat exchangers by considering their ability on
 256 remove heat from the exhaust gases. The result of this investigation is presented in
 257 Figure 6. As it is can be evidenced, the addition of an extra heat exchanger with the same
 258 characteristics of the original one allows to remove a significant additional quantity of
 259 heat from the EGR. Nonetheless, further increase of heat exchangers does not provide
 260 any appreciable benefit on EGR cooling. In this sense, the new heat exchanger proposal
 261 has considered the use of two heat exchangers in series (the original plus an extra one).
 262 This system was used for both the HP EGR system and EGR e-pump system.



263

264

Figure 6. Performance of different number of heat exchangers in the EGR circuit.

265

2.3.2. Numerical analysis

266

267

268

269

270

271

272

273

274

275

A numerical analysis is also proposed to assess the influence of the e-pump EGR system on different driving scenarios. To do this, a mild hybrid platform was designed considering the methodology proposed by García et al.[33] A Volvo FE 350 truck was used, since it is originally equipped with the engine used in these investigations [34]. Battery size and electrical motors were defined by means of an optimization process. Details about the design process can be verified in García et al [33][35]. Figure 7 illustrates the final truck architecture containing the modifications for accommodating the DMDF combustion and the mild hybridization. Two fuel tanks are included in the system as well as a small battery pack and a belt assisted starter (BAS). The main characteristics of the truck platform are presented in Table 4.

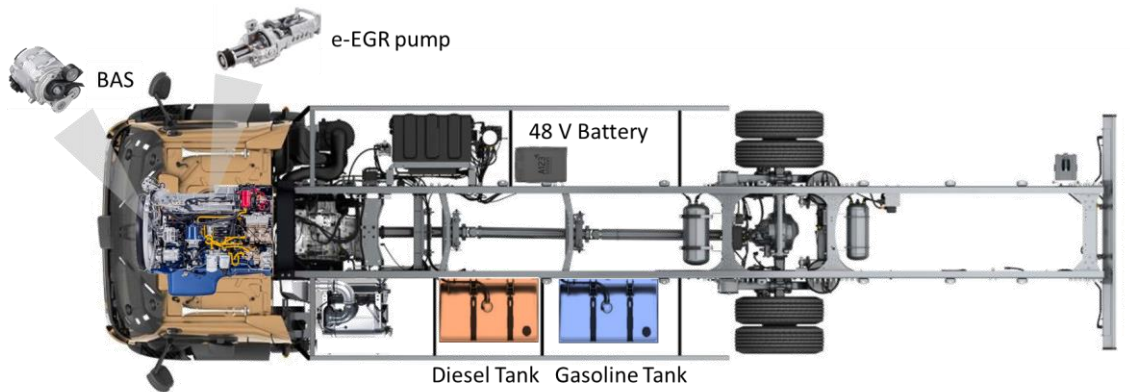


Figure 7. Schematic of the vehicle modifications assumed for the mild hybrid architecture.

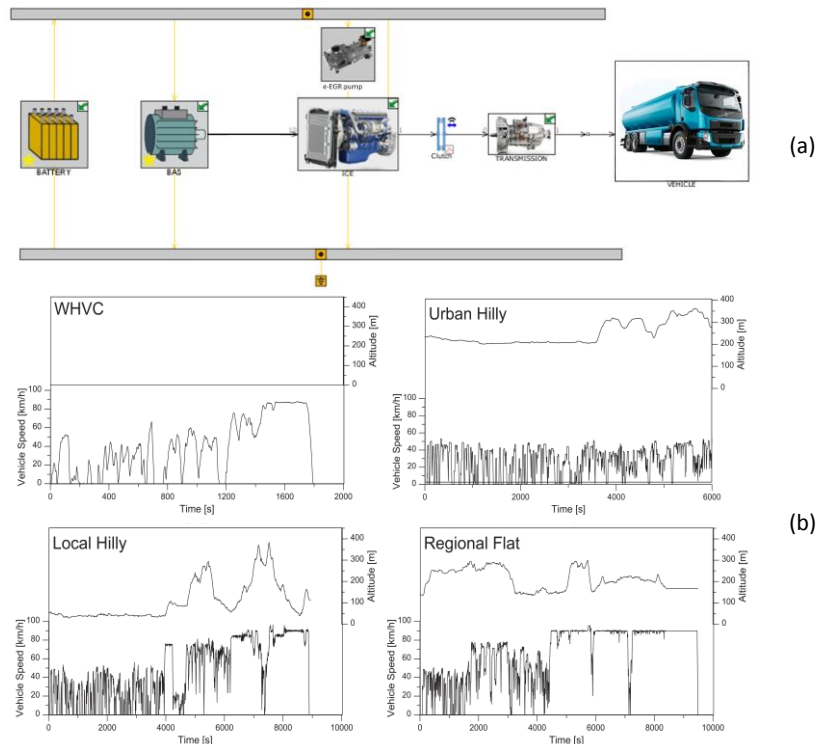
Table 4. Main characteristics of the vehicle model and electric components.

Characteristic	Value
Base vehicle Mass [kg]	7035
Max Payload [kg]	8982.5
Frontal Area [m ²]	6.89
Tires Size [mm/%/inch]	295/80/22.5
Gear Box type [-]	12 gears manual
Differential ratio [-]	3.08
ICE rated power [hp]	350@2200rpm
ICE rated Torque [Nm]	1400
Battery size [kWh]	2
Electric motor size [kW]	22.4

280

281 A 0-D numerical model was built in GT-Drive to enable the simulation of different driving
 282 cycles and payloads with and without EGR e-pump and the comparison to the
 283 conventional truck architectures such as the conventional diesel combustion and the
 284 DMDF. The final model is represented in Figure 8. As it can be seen, it consists of
 285 different objects that represent the components of the truck. The ICE object allows the
 286 use of the experimental fuel consumption and emission maps as inputs to the
 287 simulation. This approach has demonstrated the capability of reproducing transient
 288 results with good accuracy [36][37]. In addition to the ICE object, other components
 289 such as the battery model, BAS, transmission, and vehicle geometry are defined in the
 290 remaining objects. An explicit solution scheme is used to integrate the differential
 291 equations with respect to time whereas different integrators are used to obtain the
 292 cumulative results regarding fuel consumption and emissions [38]. The simulation was
 293 performed considering four different driving cycles (flat, local, urban and WHVC) and
 294 three different truck payloads (0%, 50% and 100%). The selected driving cycles are
 295 representative of both in-service conformity and normative driving cycles, while the
 296 payload of 50% is the payload used for homologation purposes [39].

297



298 Figure 8. Schematic of the vehicle architecture implemented in GT-Drive (a) and the different driving scenarios
 299 considered for the study (b).

300 3. Results and discussion

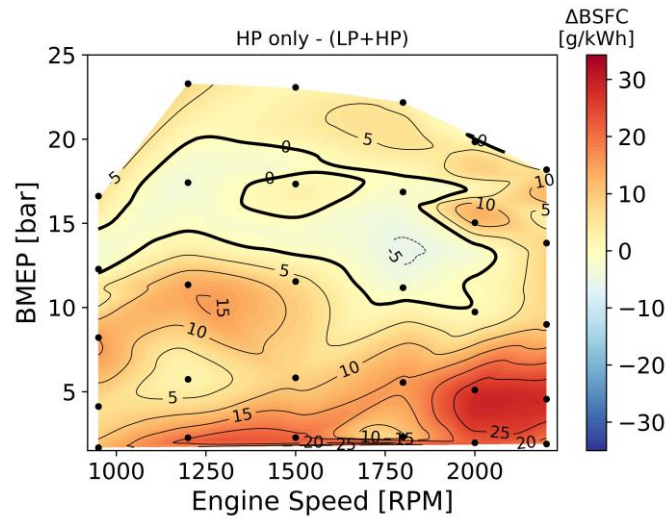
301 The results section is divided into different parts. First, the simplification of the original
 302 DMDF EGR system by removing the low pressure EGR circuit and the assessment of its
 303 impact on performance and emissions is presented. Next, the effect of introducing the
 304 EGR e-pump system is discussed from a combustion, performance, and emissions basis.
 305 Finally, a full map calibration considering the EGR e-pump as the preferred alternative
 306 to drive EGR is proposed, followed by the assessment of the calibration maps in a mild
 307 hybrid electric vehicle (MHEV) and its comparison to the conventional DMDF and diesel
 308 combustion concepts in a conventional powertrain architecture.

309 3.1. Simplifying the EGR circuit: removing the low pressure EGR

310 Prior to any evaluation with the EGR e-pump system, preliminary investigations were
 311 done removing the low pressure EGR system to understand the impact of using this
 312 simplified approach and to set a benchmark to be used as comparison for the electrified
 313 architecture. As previously commented, this approach would benefit the application of
 314 the engine architecture in terms of packaging and production costs. In this sense, a full
 315 map calibration was performed using the HP EGR system. The results for performance
 316 and emissions were then compared with those from the LP + HP pressure EGR system
 317 reported in previous results.

318 Figure 9 presents the brake specific fuel consumption (BSFC) results obtained with the
 319 new EGR configuration compared to the original LP + HP EGR circuit. As it is shown, the
 320 removal of the low pressure EGR circuit leads to penalizations in fuel consumption in
 321 most of the cases, with absolute fuel consumption increases of up to 25 g/kWh. These
 322 results are a consequence of the higher pumping losses that are obtained with the new

323 EGR configuration, since the exhaust gas are derived prior to the turbine, requiring it to
324 work in closed VGT positions and low efficiency points. This is mainly perceived from low
325 to medium load conditions. As the load is increased, the differences are also lower since
326 the exhaust gases energy availability allows to have better operating conditions inside
327 of the turbine.

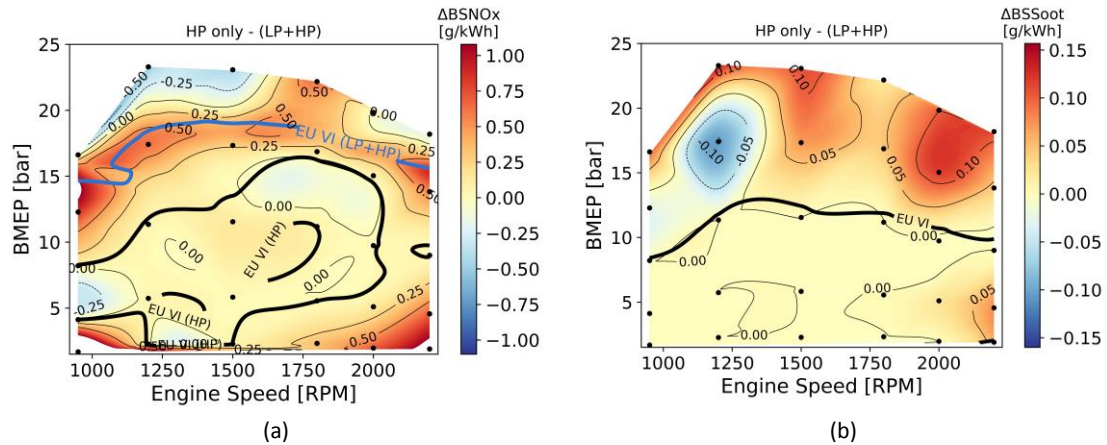


328

329 Figure 9. Differences in BSFC between the dual-route EGR architecture and the single-path EGR architecture.

330 It should be also remarked that the calibration strategies from both architectures is not
331 the same. While the LP+HP EGR system aims at obtaining EUVI NO_x values with ultra-
332 low soot, the new HP system cannot comply with this strategy. Therefore, the calibration
333 with HP EGR was a compromise between fuel consumption optimization and low NO_x
334 and soot emissions. However, as it is depicted in Figure 10 (a), the region where EUVI
335 legislation is fulfilled is much lower than that from the LP+HP EGR calibration considering
336 NO_x emissions. While the original calibration was able to fulfill the EUVI targets in terms
337 of NO_x up to 80% of engine load, the HP EGR calibration has only a narrow zone located
338 in the middle speed middle load conditions. This is a consequence of higher inlet
339 temperatures that are obtained with the new EGR system since the heat flow through
340 the EGR heat exchanger increases, even with the additional heat exchanger system.
341 Moreover, the low pressure EGR system cooling effect is not present anymore. Both
342 reasons contribute to higher inlet temperatures and consequent higher NO_x formation.
343 By contrast, the ultra-low soot emission zone (soot < 10 mg/kWh) seems to not be
344 significantly affected by the EGR system modification (Figure 10 (b)).

345 From this analysis, it can be concluded that the removal of LP EGR system does not bring
346 any benefit in terms of neither emissions nor fuel consumption. In this scenario, the use
347 of strategies that may improve the EGR system operation such as the e-pump EGR
348 system are of interest. To explore this, the next sections deal with the introduction of
349 this system in the combustion concept and its evaluation using different methodologies.



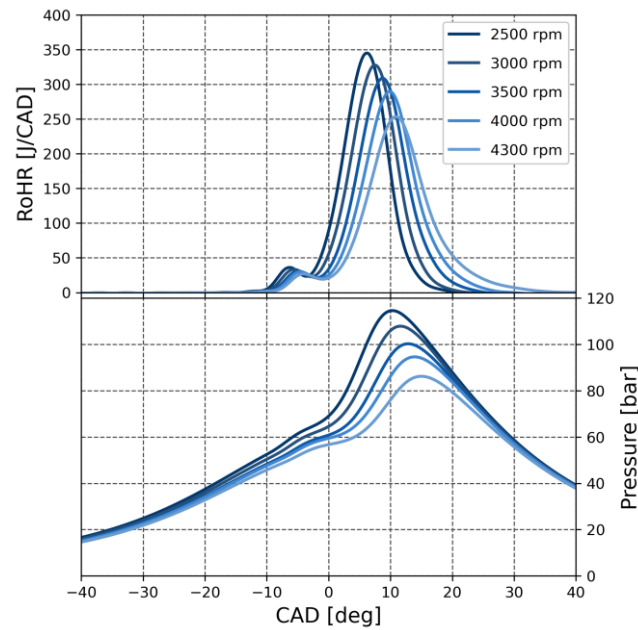
350 Figure 10. Differences in BSNO_x (a) and BSSoot (b) between the dual-route EGR architecture and the single-path EGR
 351 architecture.

352

353 3.2. EGR pump as alternative to improve engine performance.

354 As previously demonstrated, removing the LP EGR route leads to several drawbacks
 355 concerning fuel consumption and NO_x and soot emissions. Therefore, an alternative
 356 must be realized to attain a mid-term solution regarding packaging, while still offering
 357 the required boundary conditions to obtain a proper DMDF combustion. This may be
 358 attained by including the EGR e-pump system, also enabling a second route of efficiency
 359 gain by means of the energy recovery. To investigate the opportunities of improving the
 360 concept with this EGR system, a sweep-based investigation was performed, evaluating
 361 different pump speeds at 50% of engine load and several engine speeds (from 950 rpm
 362 to 2200 rpm), some of the most demanding conditions in terms of EGR and air
 363 management settings. It is important to remark that the sweeps aimed at delivering the
 364 same engine power output and EGR levels, which is obtained by tuning the VGT position.

365 Figure 11 illustrates the effect of the EGR pump speed on the combustion development
 366 by means of the heat release rates for 50% of engine load and 1800 rpm of engine speed,
 367 condition that presents one of the highest EGR levels. As it is shown, the increase of the
 368 e-pump speed leads to a delayed combustion process. This result is a consequence of
 369 the complex interplay between the air management and injection systems and their
 370 impact on the combustion development. This can be evidenced in Figure 12, where the
 371 intake and exhaust manifold pressures as well as the EGR levels and total LRF injected
 372 mass are presented. While the EGR levels are maintained constant, both intake and
 373 exhaust pressures are modified. The variation of the pump speeds requires to modify
 374 the VGT position, leading to lower exhaust pressures and a consequent different
 375 pressure ratio in the turbine. Since the compressor operation is directly impacted by the
 376 turbine settings, differences in the compressor outputs are also expected.

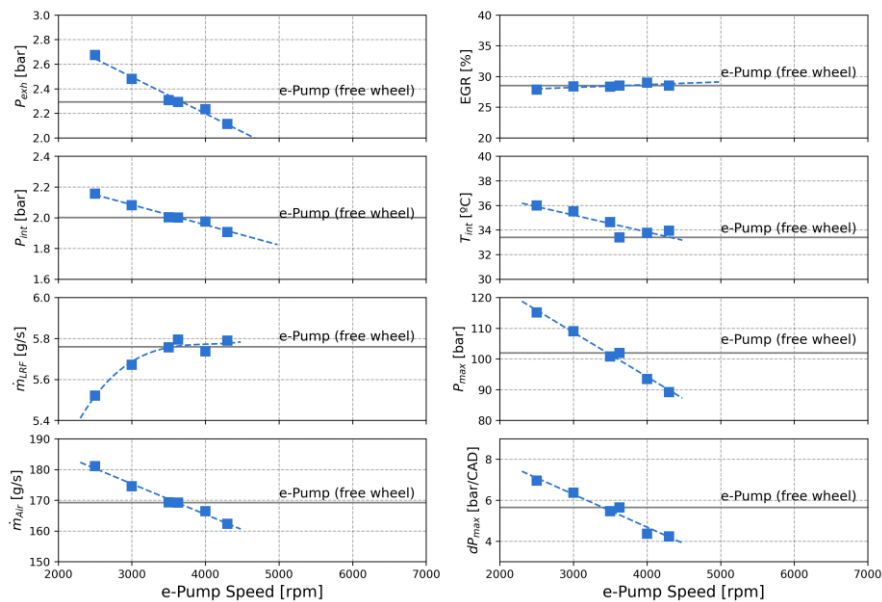


377

378

Figure 11. Effect of the EGR e-pump on in-cylinder thermodynamic evolution.

379 As it is shown also in Figure 12, despite having similar EGR and power output levels, the
 380 air management cannot deliver the same air mass flow values, which means a
 381 modification of the operating condition towards richer equivalence ratios. Despite this,
 382 the combustion seems to be negatively affected by the increase of the EGR e-pump
 383 speed. This can be explained by the decrease of both inlet pressure and temperature as
 384 the e-pump is accelerated, resulting in worse conditions for the fuel oxidation.



385

386

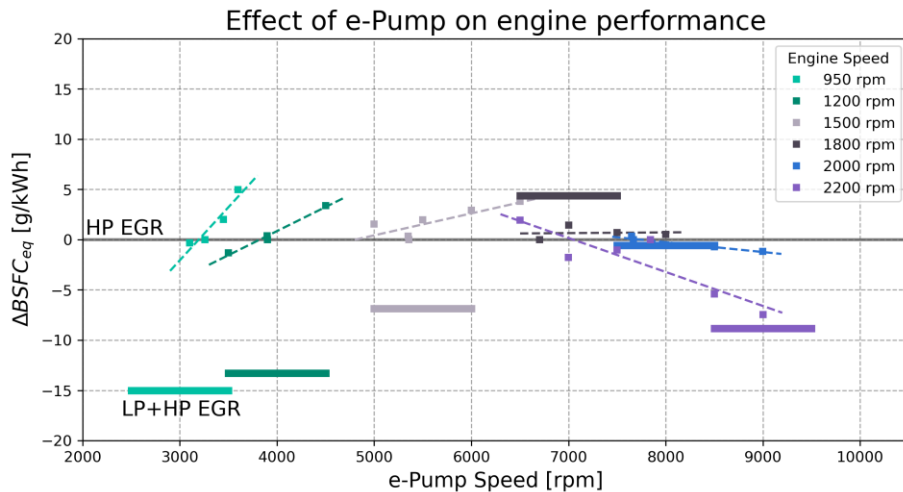
Figure 12. Effect of the EGR e-pump on different engine boundary conditions.

387 Other secondary phenomena also occur as the inlet pressure is modified. As it is shown,
 388 compression ratio reduction in the compressor modifies the total fuel mass injected by
 389 the low reactivity fuel injection system. This modification is a consequence of the higher-
 390 pressure difference between the injection pressure and the manifold pressure. This

391 phenomenon is expected to be found in real applications and therefore was not
392 corrected during the experiments since it did not impact the target variables (EGR levels
393 and power output). Lastly, the use of the EGR e-pump adds another degree of freedom
394 to mitigate maximum pressure and maximum pressure gradients within the cylinder,
395 that are directly related to noise emissions and mechanical durability of the engine. As
396 shown in Figure 12, it is possible to maintain power output and EGR levels while reducing
397 noise emissions and lowering the mechanical demand over the engine structural
398 components.

399 The use of the EGR e-pump also opens new paths to recover energy from the exhaust
400 gas. This means that this energy path must be included in the total efficiency of
401 calculation. Additionally, the variation of the air management configuration is expected
402 to have a significant influence on the pumping losses of the engine. The combination of
403 all the discussed parameters such as combustion phasing, pumping losses, fuel mass,
404 etc., will culminate in the outcome of energy conversion that is the brake specific fuel
405 consumption equivalent, presented in Eq. 1. This parameter allows to characterize the
406 global effect of the EGR e-pump, which is depicted in Figure 13. This figure summarizes
407 the effect of EGR e-pump speed for 50% of engine load and engine speeds from 950 rpm
408 to 2200 rpm considering the values from HP EGR calibration as references. Each square
409 represents the $BSFC_{eq}$ with the EGR e-pump, while the solid horizontal bars refer to the
410 reference value from the LP+HP EGR original calibration.

411 As it can be observed, there is a trend inversion regarding the effect of the pump speed
412 on the $BSFC_{eq}$ values as the engine speed is increased. At low engine speeds (950 rpm),
413 the EGR e-pump operation results in a better overall energy conversion when it is
414 operating at low speeds. This means that the pump is operating in a regenerative mode,
415 extracting energy from the flow. In general, at these conditions, an improvement on
416 $BSFC_{eq}$ of 2.5 g/kWh can be obtained. It is worth mentioning that as the methodology
417 seeks to maintain the EGR and emissions level, when the pump is regenerating energy,
418 it is necessary to further close the VGT and increase the volumetric pump inlet density
419 by means of higher pressure. To have a wider range of regeneration capacity on the e-
420 pump it would be necessary to assess the turbo-matching and sizing of the VGT to
421 ensure that there is enough margin to maneuver with the rack position. As the engine
422 speed is increased, the trend starts to invert towards higher EGR e-pump speeds,
423 meaning that the most advantageous operation comes from providing energy to the
424 EGR flow. This enables the decrease of the pumping losses of the engine by means of
425 opening the VGT rack position. This type of operation can provide benefits of up to 8
426 g/kWh, much higher than those when the EGR e-pump works at regenerative mode. It
427 is also worth to mention that, in most of the cases, the introduction of the EGR e-pump
428 system allows to have better $BSFC_{eq}$ results than those from the HP EGR system.
429 Additionally, at high engine speeds, the improvements can be higher enough to achieve
430 almost the same $BSFC_{eq}$ results than those from the dual-route EGR system. In this sense,
431 it can be concluded that the addition of the EGR e-pump system can enable a more
432 efficient operation by different paths (regeneration or reduction of pumping losses).
433 Nonetheless, a wider assessment must be done to identify if the effect is preserved also
434 on other engine loads. To do this, a full map calibration is proposed in the next
435 subsection.



436

437

Figure 13. Effect of the EGR e-pump on engine performance depending on the engine working regime.

438

3.3. Full map calibration using the EGR e-pump system

439

Considering the previous conclusions, the assessment of the EGR e-pump was extended to a full map calibration addressing 30 operating conditions (10%, 25%, 50%, 75%, 100% at 950 rpm, 1200 rpm, 1500 rpm, 1800 rpm, 2000 rpm and 2200 rpm). For each operating condition, the best equivalent fuel consumption value was aimed while fulfilling the restrictions in terms of NO_x and soot from the previous calibration as always as possible. Figure 14 presents the $BSFC_{eq}$ map in absolute difference basis compared to the previous HP EGR calibration. It can be inferred that the use of the EGR e-pump system allows to improve the fuel consumption in a wide extent of the calibration map. In addition is interesting to note that the improvement zone is in regions widely used during conventional driving conditions. Finally, the higher benefits are also found in high engine speeds corroborating with the results presented in Figure 13.

442

443

444

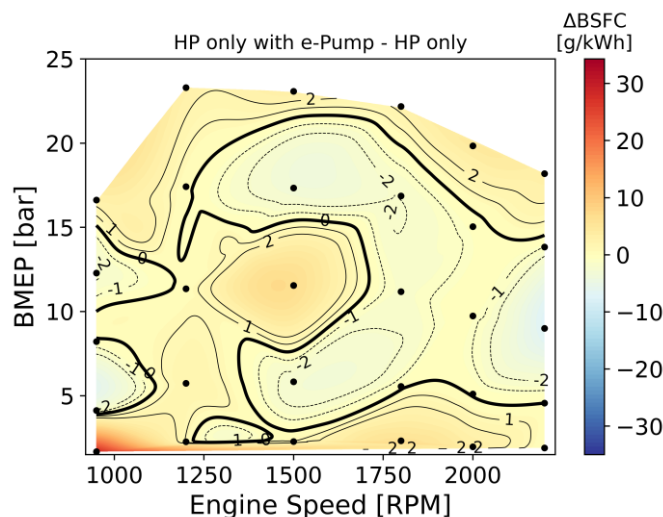
445

446

447

448

449



450

451

Figure 14. Differences in $BSFC_{eq}$ between the HP EGR architecture with and without the EGR e-pump.

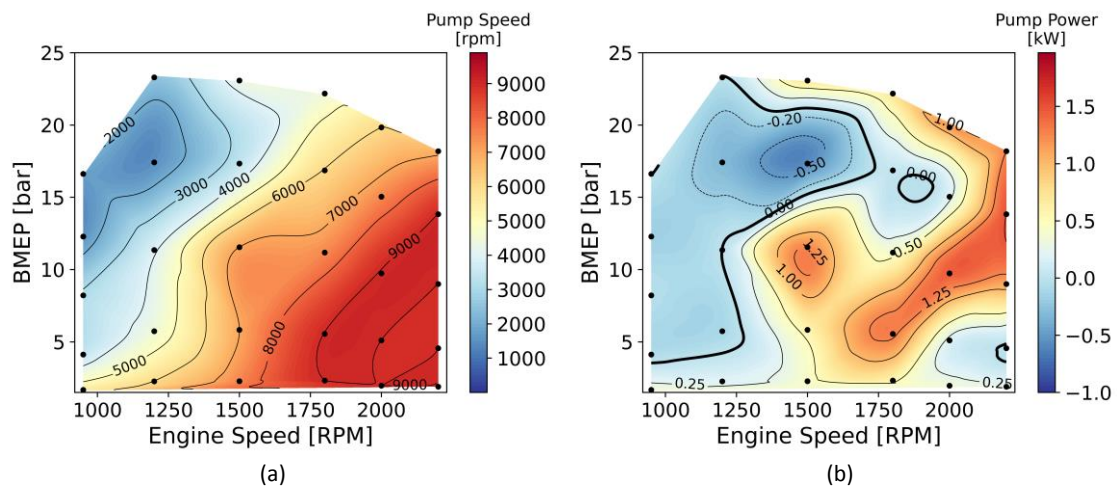
452

453

454

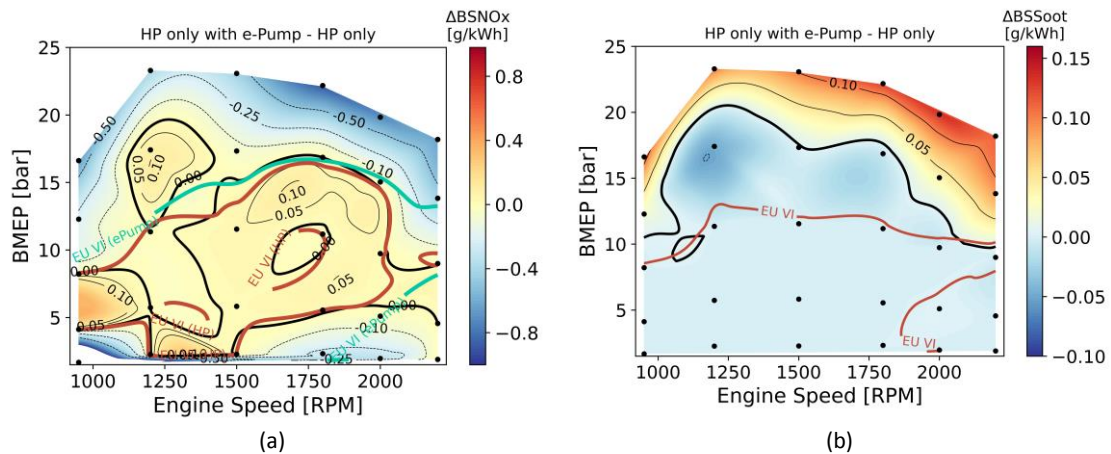
Figure 15 depicts important parameters regarding the EGR e-pump speed operation such as the pump speed and the energy flow in the pump (regeneration in negative and consumption in positive). From the analysis of Figure 15 (a), it can be inferred that the

455 e-pump velocity is scaled directly with the engine speed. Additionally, as previously
 456 commented, the powertrain benefits from higher EGR e-pump speeds as the engine
 457 speed increases. However, as shown in the Figure 15 (a), there is a wide range in the
 458 operating map where the pump works close to or in the maximum allowable speed. This
 459 allows to state that the benefits of using the pump could be extended in case of having
 460 a bigger EGR e-pump system. The analysis of the EGR e-pump power also allows to
 461 identify the possible zones where regeneration is possible. As shown in Figure 15 (b),
 462 the e-pump works regeneration mode is enhanced at low engine speeds and higher
 463 loads where the flow velocities are low, and the pumping work does not play a dominant
 464 role on the efficiency. However, as previously discussed, at high engine speeds, the e-
 465 pump is used to decrease the pumping work of the engine, providing flexibility to the
 466 turbine, and assisting to drive the EGR flow towards the intake manifold.



467 Figure 15. Operating conditions of the e-pump within the engine map in terms of pump speed (a) and power flow
 468 (b).

469 The use of the EGR e-pump system also allows to attain benefits on NO_x emissions as
 470 presented in Figure 16. The first noticeable change is the increase of the limits where
 471 engine-out tailpipe EUVI compliant NO_x emissions are obtained. Nonetheless, benefits
 472 are also evidenced at high to full load conditions. As previously stated, the use of higher
 473 EGR e-pump speeds leads to a decrease of the temperature and pressure at the inlet
 474 valve close, affecting the combustion process evolution. The simultaneous analysis of
 475 NO_x and soot emission maps allows to garner relevant information about the benefits
 476 and limitations of the EGR e-pump regarding these pollutants. As it is shown in the soot
 477 maps, the apparent benefits in NO_x emissions near to full load operation has as
 478 consequence a further increase on soot emissions compared to the original HP EGR
 479 calibration. This may be justified due to the worst conditions that are attained during
 480 the combustion to oxidize the soot emission that is generated. This mechanism (soot-
 481 NO_x trade-off) is widely addressed in the literature [40]. In this sense, it can be argued
 482 that the benefits of the EGR e-pump regarding soot and NO_x emissions are limited in
 483 these zones.



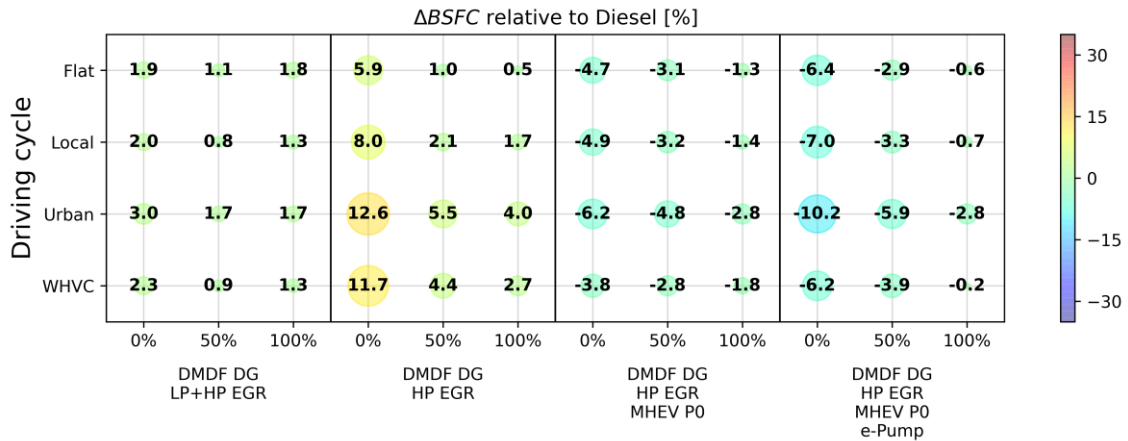
484 Figure 16. Differences in BSNO_x (a) and BSsoot (b) between the HP EGR architecture with and without the EGR e-
 485 pump including EUVI compliant regions.

486 3.4. Driving cycle assessment using the EGR e-pump system

487 Since different trends were observed in which concerns performance and emissions
 488 values, a driving cycle analysis was proposed to identify the overall performance of the
 489 EGR e-pump system on homologation and real driving conditions considering the
 490 methodological approach presented in section 2.3.2. Figure 17 presents the results of
 491 the driving cycle, comparing the results from the EGR e-pump in a mild hybrid vehicle
 492 with those from the original calibration with LP EGR and only HP EGR system in a
 493 conventional powertrain. In addition, the PO mild hybrid vehicle using the HP EGR
 494 calibration maps was also added to the system to provide a reference for the electrified
 495 version of the truck. All the results are referred to the conventional engine operating
 496 with conventional diesel combustion.

497 As Figure 17 shows, the driving cycle evaluation highlights the penalizations in BSFC_{eq}
 498 that are obtained when the LP EGR system is removed. The highest penalizations occur
 499 in urban driving conditions, where the energy requirements are low, leading to a
 500 frequent operation in low to medium load conditions. These conditions were
 501 demonstrated to be the most penalized when the LP EGR system is removed in the
 502 steady state maps. A further step was done, by including a PO MHEV architecture
 503 coupled with the HP EGR system. This architecture comprehends one of the lowest
 504 levels of electrification but allows to have electric devices such as the e-pump. As it can
 505 be seen, the electrification of the HP EGR system platform allows BSFC_{eq} improvements
 506 from $\approx -9\%$ to $\approx -18\%$, depending on the driving condition evaluated. The lowest benefits
 507 obtained for the MHEV architecture are found for driving conditions which contains
 508 highway phases. Finally, the EGR e-pump architecture is included in the model and
 509 assessed in the different driving conditions. The results allow to infer that the
 510 combination of MHEV and e-pump allows to reduce the overall vehicle equivalent fuel
 511 consumption in more than 4% for urban applications compared to the MHEV with only
 512 HP EGR. This is a direct consequence of the increase of the benefits attained in the
 513 steady state maps with the e-pump at low to medium engine load conditions. As the
 514 truck payload is increased, lower are the benefits for the MHEV architecture,
 515 independently of using or not the EGR e-pump, since most of the points are displaced
 516 towards high load operation. In this sense, it can be concluded that the proposed MHEV

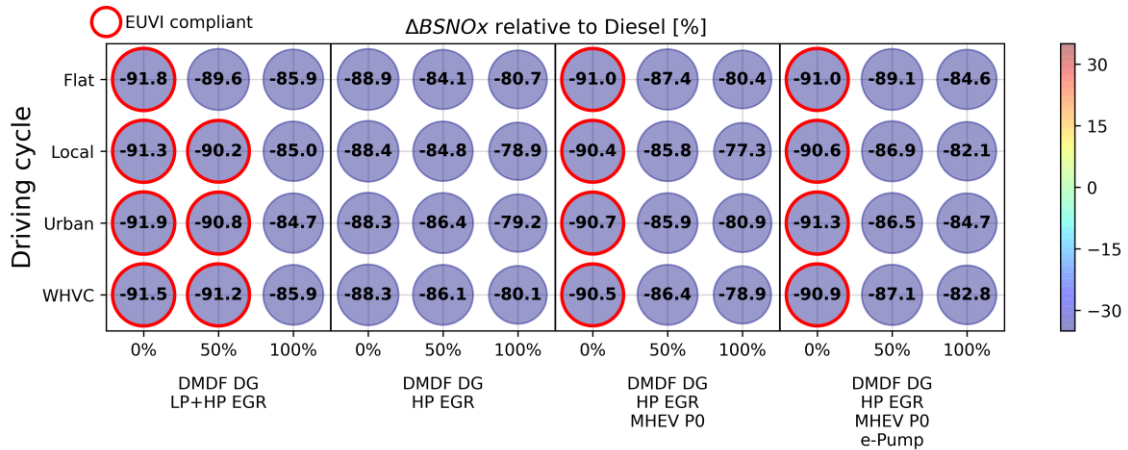
517 with EGR e-pump architecture is more suitable for urban applications rather than
 518 highway, enabling significant energy savings for this driving condition.



519

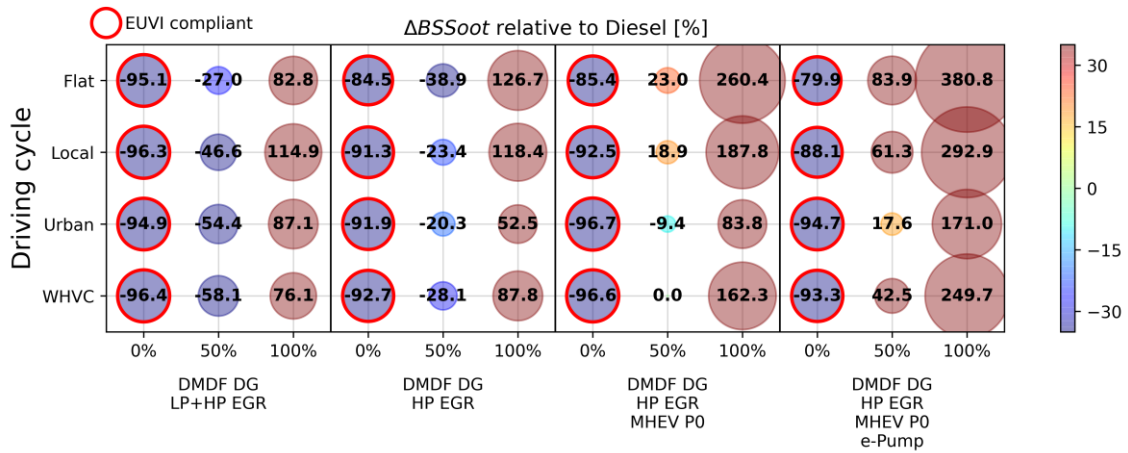
520 Figure 17. Difference in BSFC of different engine architectures compared to CDC under different driving conditions
 521 and payload.

522 The impact of the EGR e-pump on NO_x and soot emissions was also assessed considering
 523 its coupling with the MHEV architecture. Despite of the general reduction of, at least,
 524 77% in NO_x emissions due to the low temperature combustion concept, it can be
 525 evidenced that the use of the e-pump provides an overall improvement, independently
 526 on the operating condition assessed. Nonetheless, as it is shown in Figure 19, the NO_x
 527 reduction comes at the cost of increasing the soot emissions. This is enhanced as the
 528 payload increases, since the operating conditions are shifted towards high load
 529 conditions, where the soot production is significantly higher compared to the HP EGR
 530 calibration and the LP+HP EGR.



531

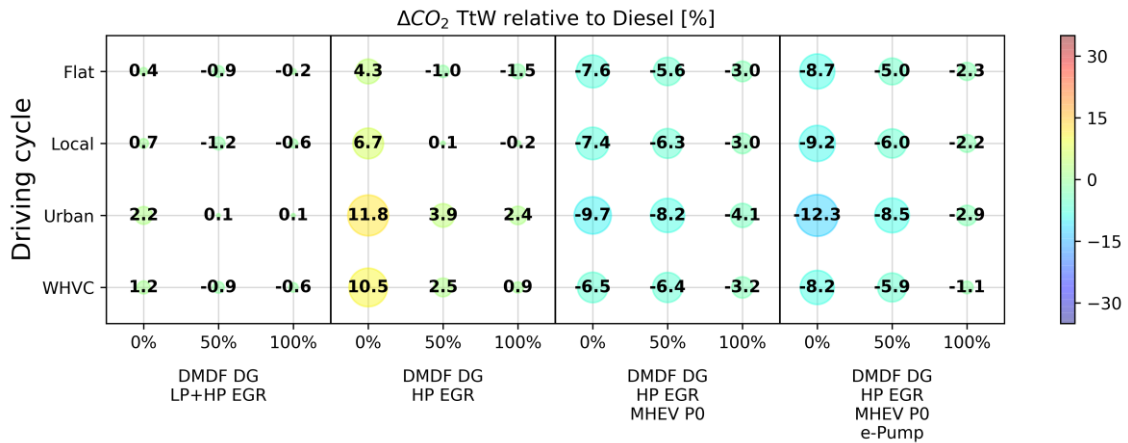
532 Figure 18. Difference in BSNO_x of different engine architectures compared to CDC under different driving conditions
 533 and payload.



534

535 Figure 19. Difference in BSSoot of different engine architectures compared to CDC under different driving conditions
536 and payload.

537 Finally, the impact of the EGR e-pump on the tank to wheel CO₂ emissions was assessed.
538 As presented in Figure 20, the combination of mild hybridization and the EGR e-pump
539 can provide CO₂ savings of up to 12.3%, considering applications in urban zones and with
540 0% of payload. Despite the decreasing trend of the TTW CO₂ savings with respect to the
541 truck payload, the benefits can range from 12.3% up to 8.5% for 0% to 50% of payload,
542 which is representative of the truck payloads in urban applications. In this sense, it can
543 be concluded that the use of the EGR e-pump system is an effective solution for
544 advanced combustion concepts offering a pathway of saving fuel consumption and CO₂
545 emissions.



546

547 Figure 20. Difference in CO₂ emissions of different engine architectures compared to CDC under different driving
548 conditions and payload.

549 4. Conclusions

550 This work has performed a detailed investigation regarding the application of the EGR
551 e-pump system combined with an advanced low temperature combustion concept as a
552 media to improve the energy conversion and management of the system. The main
553 findings of this investigation allowed to conclude that the electrification of the air
554 management system by means of the addition of the EGR e-pump provided an extra
555 degree of freedom to the system. Additionally, the combination with MHEV

556 architectures enhanced the benefits in terms of CO₂ emissions. The main conclusions
557 can be summarized as:

- 558 • The EGR e-pump impacts the overall system performance, modifying not only
559 the air management settings by also has secondary impacts on the fuel injection
560 system. Moreover, two main pathways of efficiency improvement were verified:
561 i) the EGR e-pump can allow lower pumping losses and ii) the pump can extract
562 energy from the exhaust gases and convert it into electrical energy to feed the
563 battery.
- 564 • The zones where each efficiency improvement is attained is highly dependent on
565 the engine speed. Low engine speeds allow operation in regeneration mode
566 while higher engine speed benefits the system by means of pumping losses
567 reduction.
- 568 • Despite the modifications verified in the air management system, the emission
569 values were not heavily impact by the introduction of the EGR e-pump. Engine
570 loads from low to medium load remained under the same constraints, while the
571 high to full load operation was governed by the soot-NO_x trade-off.
- 572 • The combination of the EGR e-pump system with MHEV has allowed to obtain
573 efficiency increments and TTW CO₂ reductions higher than 20% compared with
574 the conventional architecture running with HP only EGR system in urban
575 applications. These benefits are a direct consequence of avoiding the low load
576 zones and the improvements of fuel consumption in this region.

577 Considering the results obtained in this investigation, it is evident that the EGR e-pump
578 system is an effective way to reduce the fuel consumption and CO₂ emissions. The
579 highest benefits are attained at urban driving conditions. This is an important conclusion
580 since it is aligned with eco-innovation technologies that aims to reduce the impact of
581 transportation inside of the cities, i.e., in urban circuits. Therefore, it can be suggested
582 that the combination of EGR e-pump in DMDF combustion with mild hybridization and
583 eco-driving techniques may offer an effective way to achieve future CO₂ targets.

584 It can be concluded that the use of electrified air management systems and its
585 combination with advanced combustion concepts are a feasible pathway to fulfill with
586 the future regulations concerning criteria pollutants and CO₂. The use of this systems
587 with MHEV can be a cheaper and direct solution to decarbonize the transportation
588 sector and must be accounted in the mix of solution that is proposed for a carbon neutral
589 transportation scenario since it can also run synthetic fuels.

590 **Acknowledgements**

591 The authors thanks ARAMCO Overseas Company and VOLVO Group Trucks Technology
592 for supporting this research. The author R. Sari acknowledges the financial support from
593 the Spanish ministry of science innovation and universities under the grant “Ayudas para
594 contratos predoctorales para la formación de doctores” (PRE2018-085043). Operación
595 financiada por la Unión Europea a través del Programa Operativo del Fondo Europeo de
596 Desarrollo Regional (FEDER) de la Comunitat Valenciana 2014-2020 con el objetivo de
597 promover el desarrollo tecnológico, la innovación y una investigación de calidad.
598 Proyecto IDIFEDER/2020/34, Equipamiento para el desarrollo de plantas propulsivas

599 híbridas limpias y eficientes a través del uso de e-fuels, entidad beneficiaria Universitat
600 Politécnica de València.

601 **References**

- 602 [1] European Commission, "The European Green Deal," *Eur. Comm.*, vol. 53, no. 9,
603 p. 24, 2019, doi: 10.1017/CBO9781107415324.004.
- 604 [2] R. Hannah and R. Max, "CO₂ and Greenhouse Gas Emissions," p. 2020, 2020,
605 [Online]. Available: [https://ourworldindata.org/co2-and- other-greenhouse-gas-](https://ourworldindata.org/co2-and-other-greenhouse-gas-emissions)
606 [emissions](https://ourworldindata.org/co2-and-other-greenhouse-gas-emissions).
- 607 [3] European Environment Agency, "GHG emissions by sector in the EU-28, 1990-
608 2016.," 2018. [https://www.eea.europa.eu/data-and-maps/daviz/ghg-emissions-](https://www.eea.europa.eu/data-and-maps/daviz/ghg-emissions-by-sector-in#tab-chart_1)
609 [by-sector-in#tab-chart_1](https://www.eea.europa.eu/data-and-maps/daviz/ghg-emissions-by-sector-in#tab-chart_1).
- 610 [4] IEA, "Global EV Outlook 2021 - Accelerating ambitions despite the pandemic,"
611 *Glob. EV Outlook 2021*, 2021.
- 612 [5] D. Smith *et al.*, "Medium-and Heavy-Duty Vehicle Electrification: An Assessment
613 of Technology and Knowledge Gaps," no. December 2019, p. 85, 2019.
- 614 [6] M. El Hannach, P. Ahmadi, L. Guzman, S. Pickup, and E. Kjeang, "Life cycle
615 assessment of hydrogen and diesel dual-fuel class 8 heavy duty trucks," *Int. J.*
616 *Hydrogen Energy*, vol. 44, no. 16, pp. 8575–8584, 2019, doi:
617 10.1016/j.ijhydene.2019.02.027.
- 618 [7] J. Kurtz, M. Peters, M. Muratori, and C. Gearhart, "Renewable Hydrogen —
619 Economically Viable," *IEEE Electrifi. Mag.*, no. March, pp. 8–18, 2018.
- 620 [8] S. Deutz *et al.*, "Cleaner production of cleaner fuels: Wind-to-wheel-
621 environmental assessment of CO₂-based oxymethylene ether as a drop-in fuel,"
622 *Energy Environ. Sci.*, vol. 11, no. 2, pp. 331–343, 2018, doi: 10.1039/c7ee01657c.
- 623 [9] J. Benajes, A. García, J. Monsalve-Serrano, and S. Martínez-Boggio, "Potential of
624 using OMEx as substitute of diesel in the dual-fuel combustion mode to reduce
625 the global CO₂ emissions," *Transp. Eng.*, vol. 1, no. January, p. 100001, 2020,
626 doi: 10.1016/j.treng.2020.01.001.
- 627 [10] D. A. Kuhrt, E. Kühn, A. Zafiriou, and P. D. C. Küchen, "THE CONCEPT OF
628 EFFICIENCY IN THE GERMAN CLIMATE POLICY DEBATE ON ROAD TRANSPORT:A
629 comprehensive approach to assessing the efficiency of technologies," *Front.*
630 *Econ.*, no. November, 2020.
- 631 [11] E. Commission, "The optimal vehicle electri fication level in a battery-
632 constrained future," vol. 30, no. 1, 2021.
- 633 [12] F. Ueckerdt, C. Bauer, A. Dirnaichner, J. Everall, R. Sacchi, and G. Luderer,
634 "Potential and risks of hydrogen-based e-fuels in climate change mitigation,"
635 *Nat. Clim. Chang.*, vol. 11, no. 5, pp. 384–393, 2021, doi: 10.1038/s41558-021-
636 01032-7.
- 637 [13] M. Krishnamoorthi, R. Malayalamurthi, Z. He, and S. Kandasamy, "A review on
638 low temperature combustion engines: Performance, combustion and emission

- 639 characteristics," *Renew. Sustain. Energy Rev.*, vol. 116, no. October, p. 109404,
640 2019, doi: 10.1016/j.rser.2019.109404.
- 641 [14] V. B. Pedrozo, I. May, and H. Zhao, "Exploring the mid-load potential of ethanol-
642 diesel dual-fuel combustion with and without EGR," *Appl. Energy*, vol. 193, pp.
643 263–275, 2017, doi: 10.1016/j.apenergy.2017.02.043.
- 644 [15] A. García, J. Monsalve-Serrano, R. Lago Sari, and P. Gaillard, "Assessment of a
645 complete truck operating under dual-mode dual-fuel combustion in real life
646 applications: Performance and emissions analysis," *Appl. Energy*, vol. 279, no.
647 September, p. 115729, 2020, doi: 10.1016/j.apenergy.2020.115729.
- 648 [16] J. Benajes, A. García, J. Monsalve-Serrano, and V. Boronat, "Achieving clean and
649 efficient engine operation up to full load by combining optimized RCCI and dual-
650 fuel diesel-gasoline combustion strategies," *Energy Convers. Manag.*, vol. 136,
651 pp. 142–151, 2017, doi: 10.1016/j.enconman.2017.01.010.
- 652 [17] V. Macián, J. Monsalve-Serrano, D. Villalta, and Á. Fogué-Robles, "Extending the
653 potential of the dual-mode dual-fuel combustion towards the prospective EURO
654 VII emissions limits using gasoline and OME_x," *Energy Convers. Manag.*, vol. 233,
655 no. December 2020, 2021, doi: 10.1016/j.enconman.2021.113927.
- 656 [18] J. Benajes, A. García, J. Monsalve-Serrano, and R. Sari, "Clean and efficient dual-
657 fuel combustion using OME_x as high reactivity fuel: Comparison to diesel-
658 gasoline calibration," *Energy Convers. Manag.*, vol. 216, no. May, p. 112953,
659 2020, doi: 10.1016/j.enconman.2020.112953.
- 660 [19] J. Benajes, A. García, J. Monsalve-Serrano, and S. Martínez-Boggio,
661 "Optimization of the parallel and mild hybrid vehicle platforms operating under
662 conventional and advanced combustion modes," *Energy Convers. Manag.*, vol.
663 190, no. April, pp. 73–90, Jun. 2019, doi: 10.1016/j.enconman.2019.04.010.
- 664 [20] M. Alshammari, F. Alshammari, and A. Pesyridis, "Electric boosting and energy
665 recovery systems for engine downsizing," *Energies*, vol. 12, no. 24, 2019, doi:
666 10.3390/en12244636.
- 667 [21] A. García, J. Monsalve-serrano, S. Martinez-boggio, and P. Gaillard, "Emissions
668 reduction by using e-components in 48 V mild hybrid trucks under dual-mode
669 dual-fuel combustion," *Appl. Energy*, vol. 299, no. May, p. 117305, 2021, doi:
670 10.1016/j.apenergy.2021.117305.
- 671 [22] E. M. Smith, "Electrified Heavy-Duty 4-cylinder Engine Concept for Class 8
672 Trucks," *SAE Tech. Pap.*, no. 2021, pp. 1–7, 2021, doi: 10.4271/2021-01-0719.
- 673 [23] J. Benajes, A. García, J. Monsalve-Serrano, and R. Lago Sari, "Experimental
674 investigation on the efficiency of a diesel oxidation catalyst in a medium-duty
675 multi-cylinder RCCI engine," *Energy Convers. Manag.*, vol. 176, no. July, pp. 1–
676 10, 2018, doi: 10.1016/j.enconman.2018.09.016.
- 677 [24] A. García, A. Gil, J. Monsalve-Serrano, and R. Lago Sari, "OME_x-diesel blends as
678 high reactivity fuel for ultra-low NO_x and soot emissions in the dual-mode dual-
679 fuel combustion strategy," *Fuel*, vol. 275, no. February, p. 117898, 2020, doi:

- 680 10.1016/j.fuel.2020.117898.
- 681 [25] V. Macián, J. Monsalve-Serrano, D. Villalta, and Á. Fogué-Robles, "Extending the
682 potential of the dual-mode dual-fuel combustion towards the prospective EURO
683 VII emissions limits using gasoline and OME_x," *Energy Convers. Manag.*, vol. 233,
684 no. February, 2021, doi: 10.1016/j.enconman.2021.113927.
- 685 [26] J. Benajes, J. V. Pastor, A. García, and J. Monsalve-Serrano, "An experimental
686 investigation on the influence of piston bowl geometry on RCCI performance
687 and emissions in a heavy-duty engine," *Energy Convers. Manag.*, vol. 103, pp.
688 1019–1030, 2015, doi: 10.1016/j.enconman.2015.07.047.
- 689 [27] A. García, J. Monsalve-Serrano, D. Villalta, R. Lago Sari, V. Gordillo Zavaleta, and
690 P. Gaillard, "Potential of e-Fischer Tropsch diesel and oxymethyl-ether (OME_x)
691 as fuels for the dual-mode dual-fuel concept," *Appl. Energy*, vol. 253, 2019, doi:
692 10.1016/j.apenergy.2019.113622.
- 693 [28] Y. Park and C. Bae, "Experimental study on the effects of high/low pressure EGR
694 proportion in a passenger car diesel engine," *Appl. Energy*, vol. 133, pp. 308–
695 316, 2014, doi: 10.1016/j.apenergy.2014.08.003.
- 696 [29] Y. Chao *et al.*, "Comparison of Fuel Economy Improvement by High and Low
697 Pressure EGR System on a Downsized Boosted Gasoline Engine," *SAE Tech. Pap.*,
698 vol. 2017-March, no. March, 2017, doi: 10.4271/2017-01-0682.
- 699 [30] Eaton, "TVS technology overview." [https://www.eaton.com/us/en-
700 us/products/engine-solutions/superchargers/tvs-overview.html](https://www.eaton.com/us/en-us/products/engine-solutions/superchargers/tvs-overview.html).
- 701 [31] A. García, J. Monsalve-Serrano, D. Villalta, and R. Lago Sari, "Performance of a
702 conventional diesel aftertreatment system used in a medium-duty multi-
703 cylinder dual-mode dual-fuel engine," *Energy Convers. Manag.*, vol. 184, no.
704 February, pp. 327–337, Mar. 2019, doi: 10.1016/j.enconman.2019.01.069.
- 705 [32] J. Benajes, A. García, J. Monsalve-Serrano, I. Balloul, and G. Pradel, "An
706 assessment of the dual-mode reactivity controlled compression
707 ignition/conventional diesel combustion capabilities in a EURO VI medium-duty
708 diesel engine fueled with an intermediate ethanol-gasoline blend and biodiesel,"
709 *Energy Convers. Manag.*, vol. 123, pp. 381–391, 2016, doi:
710 10.1016/j.enconman.2016.06.059.
- 711 [33] A. García, J. Monsalve-Serrano, S. Martinez-Boggio, P. Gaillard, O. Poussin, and
712 A. A. Amer, "Dual fuel combustion and hybrid electric powertrains as potential
713 solution to achieve 2025 emissions targets in medium duty trucks sector,"
714 *Energy Convers. Manag.*, vol. 224, no. June, p. 113320, 2020, doi:
715 10.1016/j.enconman.2020.113320.
- 716 [34] Volvo, "Volvo FE: Product Guide," p. 36, 2017.
- 717 [35] O. Poussin, P. Gaillard, A. Garcia, J. Monsalve-Serrano, and S. D. Martinez-
718 Boggio, "Dual-Fuel RCCI Diesel-Gasoline Hybrid Truck Concept to Achieve the
719 Future Emissions Targets," 2020.
- 720 [36] A. García, J. Monsalve-Serrano, R. Lago Sari, and P. Gaillard, "Assessment of a

- 721 complete truck operating under dual-mode dual-fuel combustion in real life
722 applications: Performance and emissions analysis,” *Appl. Energy*, vol. 279, no.
723 August, p. 115729, 2020, doi: 10.1016/j.apenergy.2020.115729.
- 724 [37] A. García, J. Monsalve-Serrano, S. Martínez-Boggio, V. Rückert Roso, and N.
725 Duarte Souza Alvarenga Santos, “Potential of bio-ethanol in different advanced
726 combustion modes for hybrid passenger vehicles,” *Renew. Energy*, vol. 150, pp.
727 58–77, 2020, doi: 10.1016/j.renene.2019.12.102.
- 728 [38] Gamma Technologies, “Vehicle_Driveline_and_HEV application manual.” 2016.
- 729 [39] The European Commission, “Commission Regulation (EU) No 582/2011,” *Off. J.*
730 *Eur. Union*, pp. 1–168, 2011.
- 731 [40] T. Li and H. Ogawa, “Analysis of the trade-off between soot and nitrogen oxides
732 in diesel-Like combustion by chemical kinetic calculation,” *SAE Int. J. Engines*,
733 vol. 5, no. 2, pp. 94–101, 2012, doi: 10.4271/2011-01-1847.

734

735 **Notation**

736 **Abbreviations**

737 BAS: Belted Alternator Starter

738 BEV: Battery Electric Vehicle

739 BSFC: Brake Specific Fuel Consumption

740 BSFC_{eq}: Equivalent Brake Specific Fuel Consumption

741 BSNO_x: Brake Specific NO_x emissions

742 BSSoot: Brake Specific Soot emissions

743 CDC: Conventional Diesel Combustion

744 CO₂: Carbon dioxide

745 DMDF: Dual Mode Dual Fuel combustion mode

746 EGR: Exhaust Gas Recirculation

747 EUVI: EURO VI legislation

748 FGT: Fixed Geometry Turbine

749 HP EGR: High pressure EGR circuit

750 ICE: Internal Combustion Engine

751 LP EGR: Low Pressure EGR circuit

752 LP+HP EGR: EGR architecture with both LP and HP circuits

753 MHEV: Mild Hybrid Electric Vehicle

- 754 NO_x: Nitrogen Oxides
- 755 RCCI: Reactivity Controlled Compression Ignition
- 756 RoHR: Rate of Heat Release
- 757 TRL: Technology Readiness Levels
- 758 VGT: Variable Geometry Turbine
- 759 WHVC: World Harmonized Vehicle Cycle
- 760